AIP | Review of Scientific Instruments

Fibre optics wavemeters calibration using a self-referenced optical frequency comb

J. Galindo-Santos, A. V. Velasco, and P. Corredera

Citation: Review of Scientific Instruments **86**, 013104 (2015); doi: 10.1063/1.4904973
View online: http://dx.doi.org/10.1063/1.4904973
View Table of Contents: http://scitation.aip.org/content/aip/journal/rsi/86/1?ver=pdfcov
Published by the AIP Publishing

Fibre optics wavemeters calibration using a self-referenced optical frequency comb

J. Galindo-Santos, A. V. Velasco, and P. Corredera
Instituto de Óptica IO-CSIC, C/Serrano 121, 28006 Madrid, Spain

(Received 24 September 2014; accepted 11 December 2014; published online 12 January 2015)

Self-referenced optical frequency combs enable the measurement of optical frequencies with a very high accuracy, achieving uncertainties close to the atomic clock used as reference ($<10^{-13}$ s). In this paper, we present the technique for the measurement of laser frequencies for optical communications followed at IO-CSIC and its application to the calibration of two wavemeters in the 1.5 μm optical communication window. Calibration uncertainties down to 12 MHz and 59 MHz were obtained, respectively, for each of the devices. Furthermore, the long-term behaviour of the higher resolution wavemeter was studied during a 750 h period of sustained operation, exhibiting a dispersion in the measurements of 7.72 MHz. Temperature dependence of the device was analysed, enabling to further reduce dispersion down to a 2.15 MHz range, with no significant temporal deviations. © *2015 AIP Publishing LLC.* [http://dx.doi.org/10.1063/1.4904973]

I. INTRODUCTION

Self-referenced Optical Frequency Combs (OFC) currently provide the most accurate and reliable tool for optical frequency metrology.[1–4] An OFC is a train of pulses generated by a mode-locked laser, exhibiting equally spaced frequency modes in the spectral domain. This spectral structure, similar to a frequency ruler, is defined by two parameters: the repetition frequency, f_{rep}, set by the separation between two spectral lines (teeth) of the comb and the offset frequency, f_{CEO}, set by the distance to zero frequency of the first tooth of the comb.[5] Since f_{rep} and f_{CEO} are known with a precision only limited by the clock uncertainty, the frequency of a Laser Under Test (LUT), f_{LUT}, can be accurately measured by beating with the teeth of the OFC. For OFCs based on caesium-based atomic clocks,[6] the uncertainty in the knowledge of the frequencies of each tooth is in the range of 3×10^{-16} s.

Wavemeters (WM) used in optical communications are typically based on Michelson, Fabry-Perot, Mach-Zehnder, or Fizeau interferometers[7–9] and use an I_2 stabilized He-Ne lasers as internal reference.[10] The resolution of these instruments typically ranges between 10 MHz and 100 MHz (0.1 pm and 1 pm, respectively), with relative uncertainties on the order of 10^{-7}. Following International Bureau of Weights and Measures (BIPM) recommendations,[11] lasers locked on acetylene ($^{13}C_2H_2$) have been developed by the National Institutes of Metrology to provide calibration and traceability at telecommunication frequencies. These sources provide a reproducibility of 10^{-11} during a few hundred seconds.[12]

The Spanish National Research Council Institute of Optics (IO-CSIC, Madrid) is presently developing optical frequency standards for optical communications in the near IR region, based on an OFC referenced to the fundamental time unit (IO-OFC). In this work, we present the calibration of two WM for optical communications with this IO-OFC, as well as the characterization of their long-term performance.

II. OPERATING PRINCIPLES OF THE IO-OFC

The IO-OFC consists in a commercial mode-locked laser built upon an Er-doped fibre ring oscillator[13] (see Figure 1). The oscillator generates femtosecond pulses centred at 1560 nm, with a tunable repetition frequency between 98 MHz and 102 MHz. This repetition frequency is set by a 10 μHz resolution frequency generator (DDS120 from Menlo Systems) referenced to a Rb clock (RefGen 10491 from Time-Tech). The Rb clock exhibits a short-term stability of 10^{-13} s when linked by Global Positioning System (GPS) to the international reference. Repetition frequency is stabilized by monitoring the outputs of the frequency generator and the oscillator within a phase detector (PHD110 from Toptica). The difference between the two outputs is injected into a PID feedback loop (PID110 from Toptica), which changes the oscillator cavity length through a piezoelectric actuator.

The oscillator emission is equally split into two signals and injected into Er-fibre-doped amplifiers (labelled as Amp.1 and Amp.2 in Figure 1). Dispersion of the amplified signals is controlled through prism compressors to compensate pulse broadening. The output of the first amplifier is used for offset frequency locking by means of a f-2f interferometer stabilization unit.[14] The required supercontinuum is generated by a Highly Non-Linear Fibre (HNLF) and doubled by a non-linear crystal (PPLN) in order to beat the spectral regions around 1050 nm and 2100 nm. The resulting beat signal is detected by an InGaAs detector (FPD510-F from Menlo System) and compared to a 20 MHz reference signal in a digital phase detector (DXD200 from Menlo Systems) after filtering and amplification. The 20 MHz reference signal is generated at a reference distributor module (RFD10 from Menlo Systems), also referenced to the Rb clock. The output of the digital phase detector is injected into a PI feedback loop (PIC201 from Menlo Systems), which controls the phase in the resonator cavity by modulating the output power of the oscillator pumping

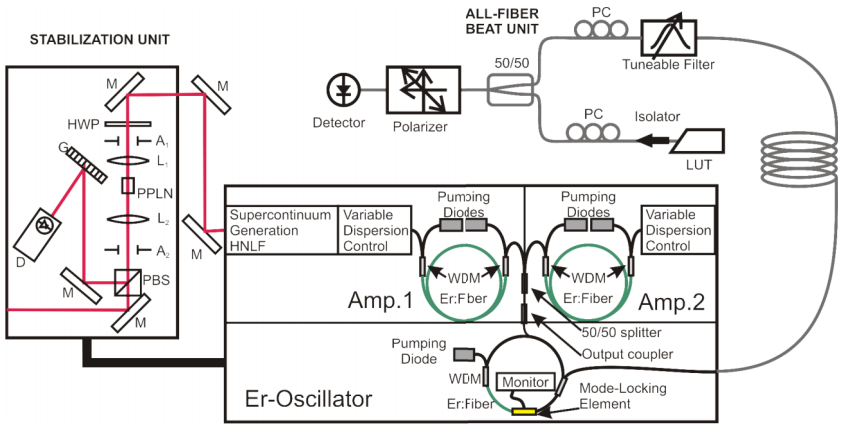

FIG. 1. Layout of the IO-OFC. WDM (Wavelength Division Multiplexing), PC (Polarization Control), M (Mirror), HWP (Half-wave plate), PBS (Polarizing beamsplitter cube), G (Grating), D (Detector), A (Apertures), L (Lens), PPLN (Lithium Niobate nonlinear crystal).

laser. The second amplifier is used for a free-space beat unit, not applied to the present work.

The IO-OFC further provides a third fibre-adapted output carrying ~6% of the oscillator optical power. This third output is used for f_{LUT} measurement by beating the LUT with the nearest OFC tooth in an all-fibre beat unit (see Figure 1). Our all-fibre beat unit consists of a tuneable optical fibre filter (JDSU TB3P, tuneable from 1460 nm to 1640 nm with $\Delta\lambda = 0.5$ nm) that selects a section of the frequency comb and two polarization controllers (PC) to adjust the polarization of the two signals before beating in a 200 MHz bandwidth InGaAs detector (FPD510 from Menlo Systems). An OSA is used for the monitorization of the relative position of the LUT and the filtered portion of the OFC to ensure correct overlapping. This design circumvents free-space alignment demands and provides tunability of the OFC output in a broader range than conventional all-fibre beat units with fixed wavelengths.

The frequencies of the optical beat signal (f_{beat}), together with electrical frequencies f_{rep} and f_{CEO}, are measured with frequency counters with 1 MHz resolution (FXM50 Menlo Systems), also referenced to the Rb clock. In order to clarify the different frequencies involved, an example of the resulting beating signal, displayed by an electric spectrum analyser (ESA), is shown in Figure 2.

For the Nth teeth of the comb, the relation of the LUT frequency and the resulting beat frequency, f_{beat}, can be expressed as

$$f_{LUT} = N \times f_{rep} \pm f_{CEO} \pm f_{beat}. \quad (1)$$

In (1), f_{beat} and f_{CEO} are positive magnitudes whose associated signs are initially unknown. Sign determination is performed by analysing the behaviour of f_{beat} to changes on the repetition frequency and offset frequency, respectively. For the determination of the value N, a previous knowledge of the LUT frequency is required, with a precision under half of the repetition frequency.

III. WAVEMETER CALIBRATION AT C-BAND OPTICAL TELECOMMUNICATION WINDOW

The described OFC was applied to the calibration of two commercial WM: EXFO model WA-1650 and Burleigh model WA-1000. Both WM are based on a Michelson interferometer with a stabilized He-Ne laser as internal reference and provide resolutions of 10 MHz and 100 MHz, respectively. The calibration of each wavemeter was carried out by simultaneous measurement and comparison of the frequency of a LUT by the wavemeter and the OFC. A 90/10 optical fibre coupler was used to feed the laser signal to both systems, with the lesser optical power being inserted to the wavemeter. Deviations in the wavemeter measurements, as characterized by the calibration procedure, are defined by its correction constant K_{fWM},

$$K_{f_{WM}} = f_{WM} - f_{OFC}, \quad (2)$$

where f_{WM} is the LUT frequency measured by the wavemeter and f_{OFC} is the same frequency measured by the OFC.

In order to perform an accurate wavemeter calibration, a stable LUT with a narrow spectrum is required. The linewidth of the LUT can be measured through heterodyne detection between the LUT and an OFC mode,[15] using an ESA. The OFC acts as a local oscillator of known linewidth (under 9 kHz), resulting in a beat signal following a Lorentzian function:

$$S_{beat}(f) = \frac{1}{1 + \left(\frac{f - f_{beat}}{(\Delta f_{LUT} + \Delta f_{OFC})/2}\right)^2}, \quad (3)$$

where S_{beat} is the beat signal spectrum recorded on the ESA and Δf_{LUT} and Δf_{OFC} are the linewidths of the LUT and

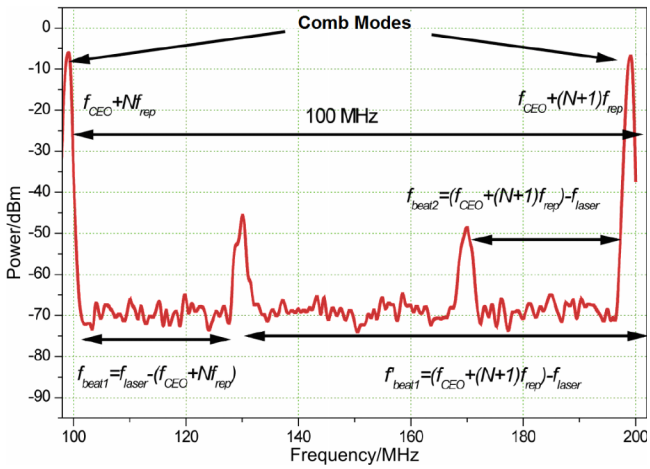

FIG. 2. Signals observed in an ESA, showing the OFC modes and the beating between OFC and the LUT.

TABLE I. Laser diodes nominal and measured linewidth.

Model	Nominal wavelength (nm)/ITU frequency (THz)	Linewidth (manufacturer) (MHz)	Linewidth (measured) (MHz)
EBLANA (EP1550-NLW-BBI-001)	1542.14/194.40	0.1	0.66 ± 0.01
EBLANA (EP1550-DM-VAD-001)	1531.90/195.80	<1	2.96 ± 0.01

the OFC mode, respectively. According to their linewidth, two lasers were selected to perform the present calibration, centred around 1532 and 1542 nm, respectively. Nominal and experimental characteristics of both sources are indicated in Table I, with ESA spectra fitting to Eq. (3) further detailed in Figure 3.

The temperature and current of selected laser diodes were controlled by a stable ILX source (model LDC-3724B). Nevertheless, this stabilization provided a limited frequency uncertainty of ±10 MHz, proving insufficient for the calibration setup. In order to achieve a greater stability, the emission of the laser sources was locked to the slope of $^{12}C_2H_2$ acetylene molecular absorption lines P11 (1531.5879 nm, EP1550-DM-VAD-001 laser) and P25 (1540.827 44 nm, EP1550-NLW-BBI-001 laser) in an NIST standard acetylene cell.[16] These molecular absorptions have been chosen to be the nearest reference available to those recommended by BIPM.

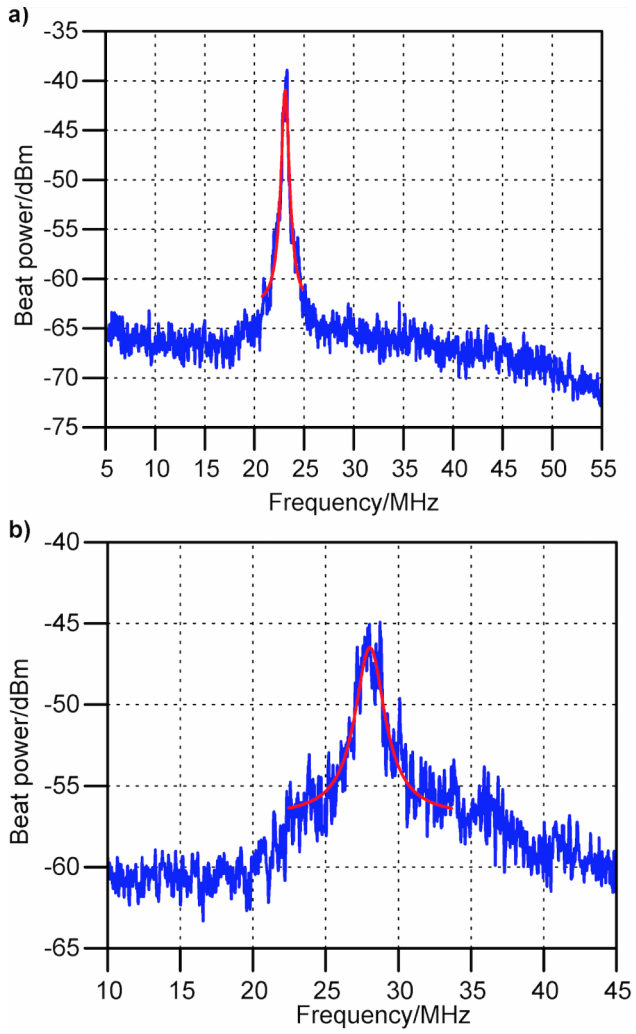

FIG. 3. ESA beating measurement (blue) and fitting to Eq. (3) (red) for linewidth characterization of laser diodes (a) EP1550-NLW-BBI-001 and (b) EP1550-DM-VAD-001.

The uncertainty in the wavemeter frequency measurement is mainly affected by the wavemeter resolution and the linewidth of the LUT, whereas the wavemeter resolution is determined by the linewidth and the frequency stability of the internal laser used as reference. However, wavemeter accuracy is also affected by the changes in the refraction index of the air path of the internal Michelson interferometer induced by changes on temperature, pressure, and humidity. Wavemeter manufactures include sensors and numerical corrections for these factors following Edlén equations,[17] but the resolution in the magnitude measurements and the precision of the correction algorithms must be taken into account. Table II shows the uncertainties in the wavemeter frequency measurement induced by these environmental effects, revealing temperature as the main limiting factor. Humidity effects are negligible in the operational wavelength range.

Uncertainty of f_{WM} is therefore affected by the statistics of the measurement, resolution of the wavemeter, linewidth of the LUT, and resolution of internal temperature, pressure, and humidity sensors. Tables III and IV detail all these factors in both wavemeters for the laser locked on line P25. Similar uncertainties result for the laser locked on line P11 in both cases.

Where type A is an evaluation of a component of measurement uncertainty by a statistical analysis of measured quantity values obtained under defined measurement conditions, and type B is an evaluation of a component of measurement uncertainty determined by means other than a Type A, as defined by the Joint Committee for Guides in Metrology (JCGM) international vocabulary.[18] The sensibility coefficient describes how the output estimate, in this case f_{WM}, changes when a small change in each input magnitude is produced and is defined by their partial derivatives at the estimation value of the input.

TABLE II. Calculation of the uncertainties of the lasers induced by dispersion of the refraction index of the air.

	Magnitude resolution	P11 (MHz)	P25 (MHz)
Temperature-related uncertainty	0.1 °C	4.36	4.34
Pressure-related uncertainty	0.1 mmHg	1.92	1.91
Humidity-related uncertainty	0.1%	0.12	0.12

TABLE III. Calculation of uncertainties of wavemeter EXFO WA-1650 for the laser stabilized on line P25 of $^{12}C_2H_2$. The uncertainties are calculated for $k = 2$.

Magnitude	Symbol	Value (Hz)	Standard uncertainty	Evaluation type	Degree of freedom	Sensibility coefficient	Uncertainty contribution (Hz)
Frequency	f	1.9457×10^{14}	0	A	5	1	0
Resolution	Δf		2.89×10^6	B	∞	1	2.89×10^6
Temperature-related uncertainty	ΔT		4.34×10^6	B	∞	1	4.34×10^6
Pressure-related uncertainty	ΔP		1.91×10^6	B	∞	1	1.91×10^6
Humidity-related uncertainty	ΔHR		1.19×10^5	B	∞	1	1.19×10^5
Laser linewidth	δ_{LUT}		1.94×10^5	B	∞	1	1.93×10^5
Σ^2							5.54×10^6
WM measured frequency	f_{WM}	1.9457×10^{14}	1.11×10^7				

TABLE IV. Calculation of uncertainties of wavemeter Burleigh WA-1000 for the laser stabilized on line P25 of $^{12}C_2H_2$. The uncertainties are calculated for $k = 2$.

Magnitude	Symbol	Value (Hz)	Standard uncertainty	Evaluation type	Degree of freedom	Sensibility coefficient	Uncertainty contribution (Hz)
Frequency	f	1.9457×10^{14}	0	A	5	1	0
Resolution	Δf		2.89×10^7	B	∞	1	2.89×10^7
Temperature-related uncertainty	ΔT		4.34×10^6	B	∞	1	4.34×10^6
Pressure-related uncertainty	ΔP		1.91×10^6	B	∞	1	1.91×10^6
Humidity-related uncertainty	ΔHR		1.19×10^5	B	∞	1	1.19×10^5
Laser linewidth	δ_{LUT}		8.54×10^5	B	∞	1	8.54×10^5
Σ^2							2.93×10^7
WM measured frequency	f_{WM}	1.9457×10^{14}	5.86×10^7				

On the other hand, the uncertainties of f_{OFC} are owing to the measurement of f_{CEO}, f_{beat}, and f_{rep}: measurement statistics, resolution of the frequency counters used (δf_{CEO}, δf_{beat}, and δf_{rep}) and uncertainties of the calibration of the counters ($\Delta f_{\text{CEO-CAL}}$, $\Delta f_{beat\text{-}CAL}$, and $\Delta f_{rep\text{-}CAL}$). It should be noted that the uncertainties associated to f_{rep} are proportional to N (~2 ×106), so in order to have a very accurate measurement of the LUT, the uncertainties related to this frequency should be as low as possible. Uncertainties derived from the laser linewidth have also been taken into account (δ_{LASER}). Tables V and VI show the uncertainties calculated for each of the two lasers, revealing LUT linewidth as the main limiting factor: 3 MHz in the case of the laser locked to line P11 and 0.66 MHz for the laser locked to line P25.

TABLE V. Calculation of uncertainties for the laser stabilized on line P11 of $^{12}C_2H_2$. The uncertainties are calculated for $k = 2$.

Magnitude	Symbol	Value (Hz)	Standard uncertainty	Evaluation type	Degree of freedom	Sensibility coefficient	Uncertainty contribution (Hz)
Repetition frequency	f_{rep}	1.0000×10^8	6.19×10^{-4}	A	1000	2.0×10^6	1.21×10^3
Counter resolution	δf_{rep}		2.89×10^{-4}	B	∞	1.0×10^8	2.89×10^4
Counter uncertainty	$\Delta f_{rep-CAL}$		1.38×10^{-2}	B	∞	2.0×10^7	2.75×10^5
Offset frequency	f_{CEO}	2.0000×10^7	7.26×10^{-2}	A	1000	1	7.26×10^{-2}
Counter resolution	δf_{CEO}		2.89×10^{-4}	B	∞	1	2.89×10^{-4}
Counter uncertainty	$\Delta f_{\text{CEO-CAL}}$		1.38×10^{-2}	B	∞	1	1.38×10^{-2}
Beat frequency	f_{beat}	2.9983×10^7	1.55×10^4	A	1000	1	1.55×10^4
Counter resolution	δf_{beat}		2.89×10^{-4}	B	∞	1	2.89×10^{-4}
Counter uncertainty	$\Delta f_{beat-CAL}$		1.38×10^{-2}	B	∞	1	1.38×10^{-2}
Laser linewidth	δ_{LUT}		1.48×10^6	B	∞	1	1.48×10^6
Σ^2 =							1.51×10^6
OFC measured frequency	f_{OFC}	1.9574×10^{14}	3.01×10^6				

TABLE VI. Calculation of uncertainties for the laser stabilized on line P25 of $^{12}C_2H_2$. The uncertainties are calculated for $k = 2$.

Magnitude	Symbol	Value (Hz)	Standard uncertainty	Evaluation type	Degree of freedom	Sensibility coefficient	Uncertainty contribution (Hz)
Repetition frequency	f_{rep}	1.0000×10^8	5.76×10^{-4}	A	1000	1.95×10^6	1.12×10^3
Counter resolution	δf_{rep}		2.89×10^{-4}	B	∞	1.0×10^8	2.89×10^4
Counter uncertainty	$\Delta f_{rep-CAL}$		1.38×10^{-2}	B	∞	2.0×10^7	2.75×10^5
Offset frequency	f_{CEO}	-2.0000×10^7	5.10×10^{-2}	A	1000	1	5.10×10^{-2}
Counter resolution	δf_{CEO}		2.89×10^{-4}	B	∞	1	2.89×10^{-4}
Counter uncertainty	$\Delta f_{\text{CEO-CAL}}$		1.38×10^{-2}	B	∞	1	1.38×10^{-2}
Beat frequency	f_{beat}	-3.0983×10^7	7.90×10^3	A	1000	1	7.90×10^3
Counter resolution	δf_{beat}		2.89×10^{-4}	B	∞	1	2.89×10^{-4}
Counter uncertainty	$\Delta f_{beat-CAL}$		1.38×10^{-2}	B	∞	1	1.38×10^{-2}
Laser linewidth	δ_{LUT}		3.35×10^5	B	∞	1	3.35×10^5
$\Sigma^2 =$							4.34×10^5
OFC measured frequency	f_{OFC}	1.9457×10^{14}	8.69×10^5				

TABLE VII. Calibrated correction constants.

Laser line	P11 $^{12}C_2H_2$	P25 $^{12}C_2H_2$
EXFO correction constant (GHz)	-0.022 ± 0.012	0.010 ± 0.011
Burleigh correction constant (GHz)	-0.090 ± 0.059	0.040 ± 0.059

For a calibration carried out at a 23 °C room temperature (34 °C internal temperature), the frequency values yielded by the OFC were 195 739.7134 ± 0.003 0 GHz (1531.587 294 ± 0.000 024 nm) for the laser stabilized in line P11 and 194 565.659 92 ± 0.000 87 GHz (1540.829 240 1 ± 0.000 006 9 nm) for line P25. Subsequent correction constants for both wavemeters are shown in Table VII. As already mentioned, the frequency uncertainty of the IO-OFC measurement is limited by the LUT linewidth, whereas the uncertainty in the WM measurement is mainly limited by the resolution of the instrument (10 MHz in the case of EXFO model WA-1650 and 100 MHz for Burleigh model WA-1000).

IV. CHARACTERIZATION UNDER LONG-TERM OPERATION

Wavemeters are commonly applied to lengthy measurements with varying temperature and pressure conditions. Therefore, a consistent behaviour under sustained operation and changing environmental factors needs to be guaranteed by the equipment. Figure 4 depicts the differences between measurements provided by the IO-OFC and the EXFO WA-1650 wavemeter for a laser source locked to the P25 acetylene line during a 750 h range with sustained wavemeter operation.

Results exhibited a significant dispersion (7.72 MHz standard deviation). While no long-term dependence to operation time was observed, measurements performed during shorter periods (up to 6 h) exhibited an increasing trend. The absence

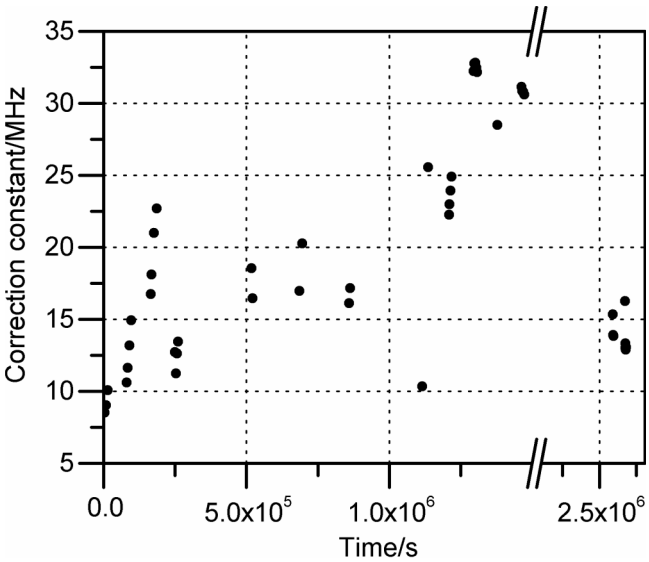

FIG. 4. Long-term variation of the discrepancy between EXFO and OFC measurements.

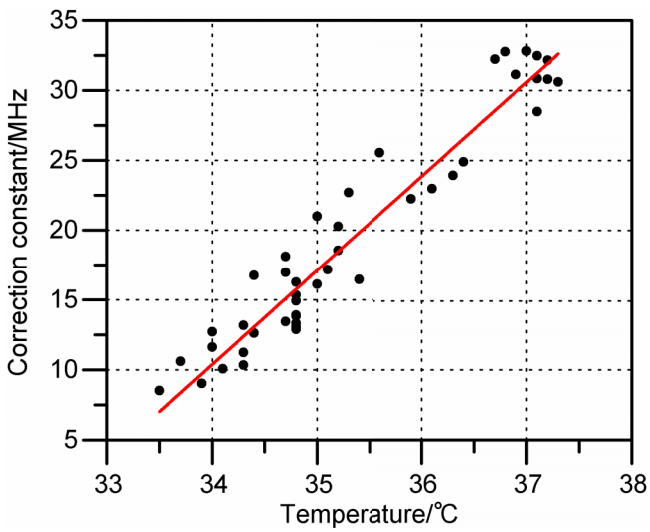

FIG. 5. Dependence of correction constant with the internal temperature of EXFO. A constant 11 °C difference between internal and external temperature of the device was maintained during the calibration process.

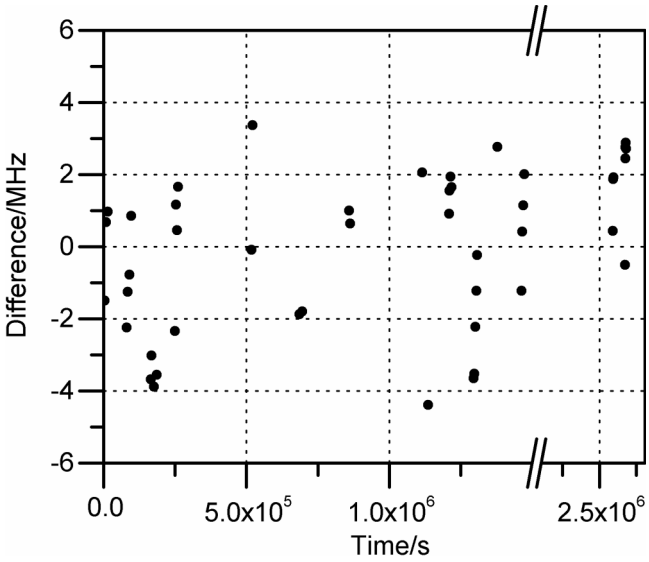

FIG. 6. Long-term variations of the discrepancy between EXFO and OFC measurements after temperature compensation.

of this trend in latter measurements, performed in the lab with a more stable temperature, pointed towards the limitations of the environmental correction algorithm of the wavemeter as the source of this behaviour. This dependence was further demonstrated by comparison of the measured correction constants and the internal temperature, T_{int}, of the device (Figure 5).

A linear trend is clearly observed, with greater discrepancies between EXFO and OFC measurements as temperature increases. This linear relation enables the numerical compensation of temperature drifts by incorporating to the calibrated correction constant, a temperature-dependent factor α,

$$K_{f_{WM}}(T_{int}) = K_{f_{WM}}(34\,^{\circ}\mathrm{C}) + \alpha\,(T_{int} - 34\,^{\circ}\mathrm{C}) = 10.382 + 6.736\cdot(T_{int} - 34\,^{\circ}\mathrm{C})\ [\mathrm{MHz}]. \quad (4)$$

After applying this compensation, the corrected wavemeter measurements become stable in the analysed 750 h lapse, as shown in Figure 6. This correction yields a time-independent standard deviation of 2.15 MHz, significantly reducing the original dispersion of 7.72 MHz.

V. CONCLUSIONS

In this paper, we have presented the laser sources characterization technique available at the IO-CSIC and its application to wavemeter calibrations for optical fibre communications in the 1.5 μm window. The disclosed technique has been applied to two laser sources stabilized in P11 and P25 absorption lines of $^{12}C_2H_2$ acetylene, respectively, proximate to ITU frequencies 195.90 THz and 194.30 THz. Lasers used in calibration were selected according to their linewidth and stability, as characterized by the IO-OFC.

With the selected lasers, the uncertainty in the IO-OFC measurement is mainly limited by LUT linewidth, whereas the uncertainty in the wavemeter measurement is mainly limited by the instrument resolution. Furthermore, temperature dependence of the higher resolution wavemeter was also characterized, enabling to further correct measurements of the device down to a 2.15 MHz dispersion range.

Finally, the long-term operation of one of the wavemeters was characterized, showing no distinguishable deviation in the measurements, provided environmental variables are maintained or numerically compensated over the duration of the measurements.

ACKNOWLEDGMENTS

This work was supported in part by the Spanish "Ministerio de Economía y Competitividad" through Project Nos. TEC2012-37958-C02-02 and TEC2012-37958-C02-01, Comunidad de Madrid through Project No. S2013/MIT-2790 and EURAMET through Project EMRP: JRP IND14 FREQUENCY.

[1]Th. Udem, R. Holzwarth, and T. W. Hänsch, Nature **416**, 233 (2002).
[2]P. Maddaloni, P. Cancio, and P. De Natale, Meas. Sci. Technol. **20**, 052001 (2009).
[3]J. Reichert, R. Holtzwarth, Th. Udem, and T. W. Hänsch, Opt. Commun. **172**, 59 (1999).
[4]S. T. Cundiff and J. Ye, *Femtosecond Optical Frequency Comb Technology* (Springer, NY, 2005).
[5]S. T. Cundiff and J. Ye, Rev. Mod. Phys. **75**, 325 (2003).
[6]T. E. Parker, Metrologia **47**, 1 (2010).
[7]C. Reiser and R. B. Lopert, Appl. Opt. **27**, 3656 (1988).
[8]H. Hussein and M. A. Sobee, Amer, Opt. Laser Eng. **48**, 393 (2010).
[9]D. Derickson, *Fiber Optic Test and Measurement* (Prentice Hall, New Jersey, 1997).
[10]A. Banerjee, U. D. Rapol, A. Wasan, and V. Natarajan, Appl. Phys. Lett. **79**, 2139 (2001).
[11]T. J. Quinn, Metrologia **40**, 103 (2003).
[12]C. S. Edwards, H. S. Margolis, G. P. Barwood, S. N. Lea, P. Gill, G. Huang, and W. R. C. Rowley, in *Conference on Precision Electromagnetic Measurements Digest 2004*, London, UK, 27 June–2 July 2004 (IEEE, 2004), pp. 668–669.
[13]F. Adler, K. Moutzouris, A. Leitenstorfer, H. Schnatz, B. Lipphardt, G. Grosche, and F. Tauser, Opt. Express **12**, 5872 (2004).
[14]D. J. Jones, S. A. Diddams, J. K. Ranka, A. Stentz, R. S. Windeler, J. L. Hall, and S. T. Cundiff, Science **288**, 635 (2000).
[15]R. Hui and M. O'Sullivan, *Fiber Optics Measurements Techniques* (Elsevier Academic Press, Burlington, MA, 2009).
[16]S. L. Gilbert and W. C. Swann, *Acetylene* $^{12}C_2H_2$ *Absorption Reference for 1510 nm to 1540 nm Wavelength Calibration-SRM2517a* (NIST Special Publication, Gaithersburg, MD, 2001), pp. 260–133.
[17]K. P. Birch and M. J. Downs, Metrologia **30**, 155 (1993).
[18]JCGM 200:2012, *International Vocabulary of Metrology - Basic and General Concepts and Associated Terms (VIM)*, 3rd ed. (JCGM, 2012).